Journal of the Korean Society for Nondestructive Testing
Vol. 23, No. 6 (2003. 12)

On Fiber Orientation Characterization of CFRP Laminate Layups Using Ultrasonic Azimuthal Scanners

Kwang-Hee Im*,†, David K. Hsu**, Jae-Gi Sim***, In-Young Yang*** and Sung-Jin Song****

Abstract Carbon-fiber reinforced plastics (CFRP) composite laminates often possess strong in-plane elastic anisotropy attributable to the fiber orientation and layup sequence. The layup orientation thus greatly influences its properties in a composite laminate. It could result in the part being rejected or discarded if the layup orientation of a ply is misaligned. A nondestructive technique would be very beneficial, which could be used to test the part after curing and to require less time than the optical test. In this paper, ultrasonic scanners were set out for different measurement modalities for acquiring ultrasonic signals as a function of in-plane azimuthal angle. The motorized scanner was built first for making transmission measurements using a pair of normal-incidence shear wave transducers. Another scanner was then built for the acousto-ultrasonic configuration using contact transducers. A ply-by-ply vector decomposition model has been developed, simplified, and implemented for composite laminates fabricated from unidirectional plies. We have compared the test results with model data. It is found that strong agreement are shown between tests and the model developed in characterizing cured layups of the laminates.

Keywords: carbon-fiber reinforced plastics (CFRP), fiber orientation, ply-by-ply vector model, defect angle, azimuthal scanner.

1. Introduction

The importance of CFRPs has been generally recognized, and CFRP composite laminates are widely used (Im et al., 2002). Increasingly more high performance engineering structures are being built with composite materials. So, CFRPs are a material class for which nondestructive material property characterization is as important as flaw detection (Hsu et al, 1994, Fisher et al, 1996, Hsu and Margetan, 1993; Hsu et al, 1997; Hale et al., 1996; Hsu, D. K. et al., (2000)). Fiber reinforced composite laminates often possess strong in-plane elastic anisotropy attributable to the specific fiber orientation and layup sequence (Tippler, 1982). However one of important factors is the layup sequence which can influence the CFRP composite performance. This greatly affects its properties in the composite laminate. If one ply is misaligned in the layup sequence, it can drastically alter the mechanical performance of composite laminates. So most manufacturers cut a small sample from the waste edge and use a microscope to optically verify the ply orientations on critical parts, which adds more cost to the composites due to intensive labor and performance after curing.

Many of these elastic anisotropies may be investigated using ultrasound, among which angular measurements are often used. An EMAT

Received: August 20, 2003. Accepted: December 7, 2003. * Department of Automotive Eng., Woosuk University, Chonbuk, 565-701 Korea ** Center for Nondestructive Evaluation, Iowa State University, Ames, Iowa 50011 USA *** Factory Automation Research Center for Parts of Vehicles and School of Mechanical Engineering, Chosun University, † Corresponding author: khim@core.woosuk.ac.kr

(electro-meganetic transducer) was used for green composite layups, sandwiched between aluminum delay lines in order to change coupling condition during the angular scan was avoided. This technique was believed to hold good potential as a practical NDE tool for detecting layup errors during the manufacturing process (Fisher, et al, 1996). Also Komsky et al. (1992) have researched the interaction of ultrasonic shear waves with thick composite laminates. This research studied the transmission of shear waves through laminates with both the transmitter and receiver aligned and fixed with respect to the fiber directions in the outer layers of the sample. Results of the experiments showed that changing the layer orientations in the laminate caused a direct effect on the received signal shape and amplitude. A layer-by-layer vector decomposition model was presented to theoretically explain the interaction of shear waves as they propagated through the laminate, but no simulated results were given for the samples tested. Also Urabe and Yomoda (Urabe and Yomoda, 1987; Yomoda, 1982) have utilized a nondestructive method using a 4 GHz microwave to determine the fiber orientation in the CFRP composites. This method is based on the electrical anisotropy in the orthotropic directions of a unidirectional laminate, with the principal direction aligned with the direction of the fibers. For this method, an incident standing wave is projected into the sample at a given orientation. The differences between the received signals, one with the receiving unit polarized horizontally and one with the receiving unit polarized vertically with respect to the apparatus, were used to determine the fiber orientation in samples constructed from two to eight plies of prepreg tape. Also, Urabe (Urabe, 1987) conducted a research using a 35GHz microwave to determine fiber orientation in carbon fiber reinforced plastics. Studies were performed on thick composite laminates by Komsky et al.(1994) . So, they have developed a method and successfully used it to predict the layer orientation for a 70-ply layer laminate through a neural network.

This paper aims at developing a motorized scanner for different measurement modalities for acquiring ultrasonic signals as a function of in-plane angle. The system is a motorized, PC-controlled angular scanner for making transmission measurements using a pair of normal-incidence shear wave transducers and investigating the inspection of ply misorientation and layup sequence in CFRP laminates when normal incident ultrasound waves transmitted in the thickness direction of composite laminates. Also an angular scan of acousto-ultrasonic signals was performed to investigate fiber reinforced composite laminates. By placing and rotating two contact transducers on the same side of crossed-plied composite laminates, the angular dependence of the acousto-ultrasonic signal was measured and found to have good correlation with the fiber orientation of the sample. Angular measurement of normal-incident shear wave has also been used to detect errors in layup sequence and ply orientation in composites. The transmitted signals of normal incident shear wave in a "crossed polarizer" configuration were found to be particularly sensitive to ply misorientation and layup sequence in a laminate. Therefore, azimuthal scan system and a new technique are presented for determining ply orientation errors and sequencing errors in a composite laminate using through transmission of shear waves based on the theoretical ply-by-ply vector decomposition.

2. Theoretical Approach

Hsu at al. (1997) suggested that a model of ply-by-ply vector decomposition decomposes the transmission of a linearly polarized ultrasound wave into orthogonal components through each ply of a laminate. The input to the first ply is decomposed into one component which propagates through the first ply parallel to the fibers and one component which propagates through the first ply perpendicular to the fibers. These two components then become the input for the second ply, where

each one is then decomposed into components parallel and perpendicular to the fibers in the second ply. This process continues for all remaining plies in the laminate.

In the derivation of the model, α_i, β_i, and ρ are the attenuation coefficient of the orientations of the transmitter, the waves polarized parallel to the fibers and the couplant layers respectively. And (h_i) is the thickness of the i^{th} ply, and (tt) and (tr) are the couplant thicknesses at the transmitter and receiver. Losses due to beam spreading and interface losses, which depend on the ply to ply orientations and thicknesses, are included in the $f_{ij}(\delta)$ signal reduction factor. The ply-by-ply vector decomposition model can now be derived.

A wave pulse, S_T, is generated by the transmitter at a transmitter angle α_T and propagates through the couplant to the face of the first ply. The wave now has the transmitter amplitude $S_T e^{-\rho(tt)}$ due to the signal attenuation of the couplant, and a time shift equal to the thickness of the couplant divided by the wave velocity through the couplant. This signal is then decomposed into two components through the change angle of each interface $\Delta\theta_1 = \alpha_T - \alpha_1$ in directions parallel and perpendicular to the fibers in the first ply. These two components shown in Fig. 1 then propagate through the first ply and are reduced by their respective attenuation, interface, and beam spreading losses. Time shifts of the two components, caused by the fact that the wave velocities, v_α and v_β are not equal, are tabulated along with the magnitude changes due to losses in lieu of the typical phase term e^{-ikx}. New values and time shifts for each component are now given by Eq. (1).

Parallel Component in 1^{st} ply at the first term of $\Delta t = (tt)/v_\rho + (h1)/v_\alpha$ (1)

$$S_{1para.} = S_T e^{-\rho(tt)} e^{-\alpha\, i(h1)} f_{11}(\delta)\cos(\Delta\theta_1)$$

Perpendicular Component in 1st ply at the first term of $\Delta t = (tt)/v_\rho + (h1)/v_\beta$

$$S_{1perp.} = S_T e^{-\rho(tt)} e^{-\beta\, i(h1)} f_{12}(\delta)\cos(\Delta\theta_1)$$

where $e^{-\alpha\, i(hi)}$ is the attenuation for the waves polarized parallel to the fibers in the i^{th} ply, $e^{-\beta\, i(hi)}$ is the attenuation for the waves polarized perpendicular to the fibers in the i^{th} ply, $e^{-\rho(tt)}$ is the signal attenuations in the couplant layers, $e^{-\rho(tr)}$ is the signal attenuations in the couplant layers, and v_α, v_β and v_ρ are the wave velocities when the component is polarized parallel to the fibers, perpendicular to the fibers, and propagating through the couplant respectively.

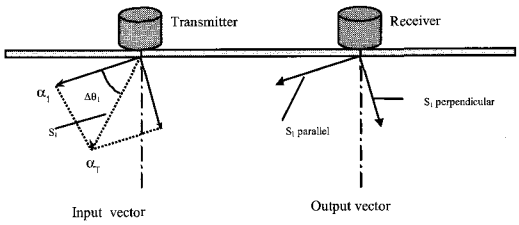

Fig. 1 Vector projection in case of input and output

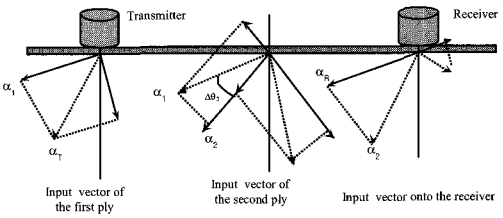

Fig. 2 Schematic of the ply to ply vector projections

As these two components enter the second ply, with the fibers oriented at α_2, each one will contribute two more components if angle α_2 does not equal angle α_1. The components are projected onto the second ply, reduced by losses, and experience another time shift as they propagate into and through the second ply, given by Eq. (2). Note that each component must retain its corresponding time shift through the calculation as shown in Fig. 2.

Parallel Components in 2nd ply at the first term of $\Delta t = (tt)/v_\rho + (h1)/v_\alpha + (h2)/v_\alpha$ (2)

$$S_{2para.} = S_T e^{-\rho(tt)} * \{e^{-\alpha 1(h1)} e^{-2(h2)} f_{11}(\delta) f_{21}(\delta) \cos(\Delta\theta_1) \cos(\Delta\theta_2) + e^{-\beta 1(h1)} e^{-\alpha 2(h2)} f_{12}(\delta) f_{24}(\delta) \sin(\Delta\theta_1) \sin(\Delta\theta_2)\}$$

Perpendicular Components in 2nd ply at the first term of $\Delta t = (tt)/v_\rho + (h1)/v_\beta + (h2)/v_\beta$:

$$S_{2perp.} = S_T e^{-\rho(tt)} * \{e^{-\beta 1(h1)} e^{-2(h2)} f_{12}(\delta) f_{22}(\delta) \cos(\Delta\theta_1) \cos(\Delta\theta_2) + e^{-\alpha 1(h1)} e^{-\beta 2(h2)} f_{11}(\delta) f_{23}(\delta) \sin(\Delta\theta_1) \sin(\Delta\theta_2)\}$$

To demonstrate the projection of the signals onto the receiver, a plate with only two plies will be used. The signal components exiting in the second ply are given in Eq. (2) and all four components will be reduced by $e^{-\rho(tr)}$ as they propagate through the couplant to the face of the receiver. The parallel component is then projected onto the receiver axis by multiplying it by cos $(\Delta\theta_R)$; likewise, the perpendicular component is projected onto the receiver axis by multiplying it by $\sin(\Delta\theta_R)$, where $\Delta\theta_R = \alpha_R - \alpha_2$. The received signal is given by Eq. (3). This equation demonstrates that the received signal is the combination of four new time varying vectors for a plate with two plies. Each new vector is constructed by multiplying the original time varying vector, S_T, by a scalar term, and shifting the new vector by its corresponding Δt.

Component parallel to receiver axis at the first term of $\Delta t = (tt)/v_\rho + (h1)/v_\alpha + (h2)/v_\alpha + (tr)/v_\rho$:

(3)

$$S_R = S_T e^{-\rho(tt)} e^{-\rho(tr)} * e^{-\alpha 1(h1)} e^{-\alpha 2(h2)} f_{11}(\delta) f_{21}(\delta) \cos(\Delta\theta_1) \cos(\Delta\theta_2) \cos(\Delta\theta_R) + e^{-\beta 1(h1)} e^{-2(h2)} f_{12}(\delta) f_{24}(\delta) \sin(\Delta\theta_1) \sin(\Delta\theta_2) \cos(\Delta\theta_R) - e^{-\alpha 1(h1)} e^{-\beta 2(h2)} f_{11}(\delta) f_{23}(\delta) \cos(\Delta\theta_1) \sin(\Delta\theta_2) \sin(\Delta\theta_R) + e^{-\beta 1(h1)} e^{-\beta 2(h2)} f_{12}(\delta) f_{22}(\delta) \sin(\Delta\theta_1) \cos(\Delta\theta_2) \sin(\Delta\theta_R)\}.$$

The ply-by-ply vector decomposition model is a very powerful tool for the ultrasonic testing of composite plates consisting of unidirectional plies. As with most theoretical methods, the ply-by-ply vector decomposition model has many complications involved with its implementation and requires that some assumptions be made to reduce it to a practical level for nondestructive testing.

3. Simplified Model

The final form for the theoretical ply-by-ply vector decomposition model, as well as similar decomposition models (Hsu et al., 1997), for a typical plate with numerous plies is a very lengthy and complex calculation. As shown previously, the number of discrete components in the theoretical model grow at an exponential rate of 2^N plate consisting of 40 plies will contribute 2^{40}, approximately 1.995 trillion, discrete terms to the calculation of S_R. An array of this size would be a highly time-consuming and inefficient computation even with the speed and power of today's computers. Another complication arises in determining the values and functions of α, β, ρ, and $f_{ij}(\delta)$ to be used in the computation of SR for many plies. In order to utilize the ply-by-ply vector decomposition technique, some assumptions and simplifications are made to simplify the theoretical model.

A plate consisting of two plies will be used to illustrate the transformation of the theoretical model to the simplified ply-by-ply vector decomposition model. The first assumption used is that the interface and beam spreading losses are negligible, that is, all $f_{ij}(\delta)$ terms equal one. This may seem to be a drastic assumption since these losses are sensitive to the order and orientation of the plies, but preliminary tests have shown this assumption to have little effect on the qualitative results and it is essential for further simplification. Next, by constraining all plies in the plate to be comprised of the same material, (h_i), α_i, and β_i are assumed to be identical for every ply. Finally, the couplant is a thin layer of highly viscous material and when the transducers

are pressed onto the plate, it is assumed that the couplant spreads into a uniform and equal thickness for both transducers; therefore, $\rho(tt) = \rho(tr) = \rho'$. The result of incorporating these assumptions into Eq. (3) and grouping like terms is given by Eq. (4) at the first term of $\Delta t = (2tt)/v_\rho + (2h)(s_\alpha)$. (4)

$$S_R = S_T e^{-2\rho'} e^{-2\alpha'} \cos(\Delta\theta_1)\cos(\Delta\theta_2)\cos(\Delta\theta_R) + S_T e^{-2\rho'} e^{-\beta'} e^{-\alpha'} \sin(\Delta\theta_1)\sin(\Delta\theta_2)\cos(\Delta\theta_R) - S_T e^{-2\rho'} e^{-\alpha'} e^{-\beta'} \cos(\Delta\theta_1)\sin(\Delta\theta_2)\sin(\Delta\theta_R) + S_T e^{-2\rho'} e^{-\beta'} \sin(\Delta\theta_1)\cos(\Delta\theta_2)\sin(\Delta\theta_R)$$

where $h=h_1, \ldots, h_N$, $\alpha' = \alpha_1(h_1), \ldots, \alpha_N(h_N)$, $\beta' = \beta_1(h_1), \ldots, \beta_N(h_N)$, $s_\alpha = 1/v_\alpha$, and $s_\beta = 1/v_\beta$.

4. Experimental Method

The CFRP composite laminates are made of 33 plies of these sheets stacked at different angles. CFRPs made from uni-directional prepreg sheets of carbon fibers (CU125NS) by Korea HANKUK Fiber Co., have the material properties shown in Table 1, based on the manufacturer's specifications. They are cured by heating to the appropriate hardening temperature (130℃) by a heater in the vaccum bag of the autoclave. A type of specimens was used in this experimentation. Its lay-up, stacked with 33 plies, indicates that specimen is $[2(90_3,0_3),90_3,\theta_3,90_3,2(0_3,90_3)]$. Here θ are defect angles (0°, 5°, 15° and 20°). Test specimens were prepared with dimensions, 70 mm × 70 mm × 4.57 mm (width × length × thickness). And the fiber-direction of specimen surface is manufactured to correspond to 0° direction; thus, the fiber-direction is the same as the length direction.

A schematic diagram of the motorized contact mode scanner is shown in Fig. 3. Two 1 MHz, 12.7 mm in diameter shear wave transducers in contact transmission mode, one of which serves as a transmitter and the other a receiver, had been used (see Fig. 4). The two transducers are supported by a holder which can be rotated by a stepper motor with a maximum resolution of 0.9 degree. Each time after a full revolution of scan, the scanner reverses to the starting position so that the cables to the transducers will not continue to wrap around the axle. Two adjustable small springs are used to maintain a certain pressure on the transducers so that the transducers are kept in contact with the sample during the transmission scan mode. The burnt honey couplant can be used for the scan. The motorized system is assembled for experimental acquisition by first placing the test specimen face down on the transmitter face plate and aligning its 90° axis between two transducers. The system consists of a PC, a pulser-receiver, a motor driver and the contact transmission mode probes described above. The parallel port of the PC is used to output the motor control signal and a high-speed data acquisition board is used to digitize the ultrasonic signals. A graphics based user interface software was developed for scan control and data analysis. With the motorized scanner, a typical transmission scan (360 degree with a step of 1.8 degree) can be done in less than one minute. Here this instrumentation included a Panametrics #5075PR pulser/receiver and a LeCroy 9400 digital oscilloscope. The waves were generated and received using a pair of Panametrics V153, 12.7 mm diameter, 1 MHz, shear wave transducers which were coupled to the composite laminates using a burnt honey couplant supplied by Panametrics. Figure 5 shows acousto-ultrasonic azimuthal scanner. Obviously it is obscure to some degree to perform the acousto-ultrasonic technique in this experimentation. However the acousto-ultrasonic technique is among alternatives that should be considered for material characterization (Vary, 1988). And acousto-ultrasonic approach is very sensitive to fiber misorientation of CFRP composites. Also we can take one-side measurement to find the effect of fiber orientation. So this system could be practically useful because of the one-side measurement which is composed of two contact mode

transducers, plunger, rubber O-ring, inner disk and hand pump. Then two L-shaped plugged transducers with 5 MHz, 6.35 mm in diameter were used to find effect of composite layup employing a pitch-catch technique. The distance between transmitter (T) and receiver (R) is 21.8 mm in spacing. Here we have manually rotated a inner ring for a turn and then reversed the ring. When turning a manual pump was used to keep the fixture holding on the measurement location. At that time we have measured peak-to-peak amplitude as a function of angle. A peak-to-peak amplitude was taken on the digital oscilloscope during data processing as shown in Fig. 6.

Table 1 Material properties

Characteristics	Fiber	Resin	Prepreg
Density	1.75×10^3 [kg/m^3]	1.24×10^3 [kg/m^3]	CU125NS
Tensile strength	3.53 [GPa]	0.078 [GPa]	
Elastic modulus	230 [GPa]	3.96 [GPa]	
Elongation	1.5 [%]	2.0 [%]	
Resin content			37 [% Wt]

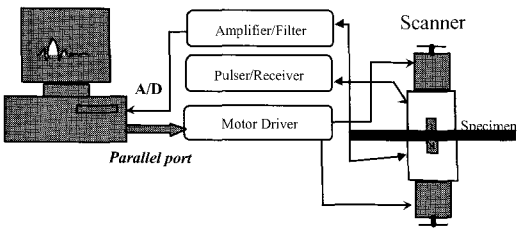

Fig. 3 Schematic for motorized scan system

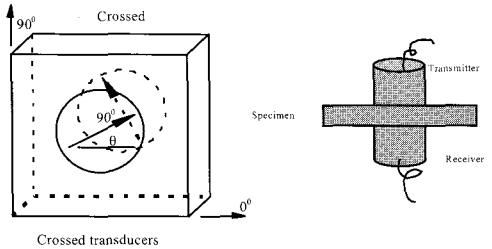

Fig. 4 Schematic of transducer contact position in through-transmission mode

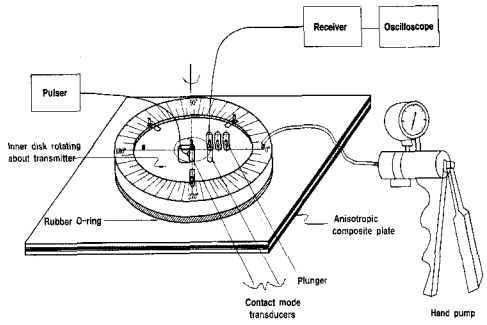

Fig. 5 Acousto-ultrasonic azimuthal scanner

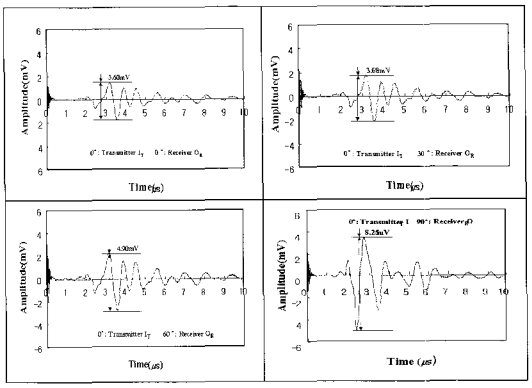

Fig. 6 Typically peak to peak amplitude of through-transmission method

5. Discussion And Results

5.1. Verification of the Simplified Model

All tests utilized a through-transmitted ultrasonic pulse which was generated and received by a pair of 1 MHz shear wave transducers. Experiments were performed on specimens fabricated from 33 plies of graphite/epoxy prepreg sheets, carbon fibers (CU125NS) by Korea HANKUK Fiber Co., with all fibers oriented parallel to each other to verify the simplified ply-by-ply vector decomposition model. An impulse signal was generated by a pulser/receiver, and the received signal was displayed on a digital oscilloscope. To verify that the reduced model worked at various transducer angles, the first set of experiments were performed using one specimen of 33 aligned

plies. This simplifies the ply-by-ply vector decomposition model to Eq. (5) below, where $\Delta\theta_1 = \alpha_T - \alpha_1$, $\Delta\theta_R = \alpha_R - \alpha_{33}$ and $R[0_{33}/90_0]$ and $R[0_0/90_{33}]$ are the experimentally acquired signals. At that time, the other 32 reference signals are not required since all of the fibers in the pack are assumed to be perfectly aligned. These terms $\sin(\Delta\theta_i)=0$, for i=2 to 33, produce coefficients equal to zero for those reference signals.

$$S_R = R[0_{33}/90_0]\cos(\Delta\theta_1)\cos(\Delta\theta_R) + R[0_0/90_{33}]\sin(\Delta\theta_1)\sin(\Delta\theta_R), \quad (5)$$

The above signals were acquired and stored in the personal computer by aligning the transducers parallel to the fibers for $R[0_{33}/90_0]$ and perpendicular to the fiber for $R[0_0/90_{33}]$. The transmitter and receiver were then oriented at specified angles, α_T and α_R, to the fibers and the received signal for each orientation was acquired and stored in the computer. A spreadsheet was utilized to model the received signal from the stored reference signals and the transducer orientations using Eq. (5). Fig. 7 shows a comparison of the received signal and the modeled signal. The slight differences in amplitudes can be attributed to a change of couplant conditions and ply orientation errors due to small random layup errors. This good agreement between the experimental and modeled wave forms verifies the simplified model.

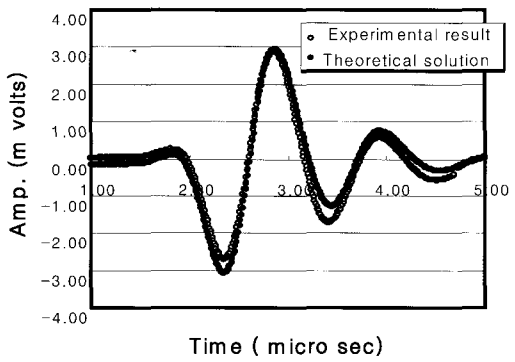

Fig. 7 Comparisons of modeling and experimental solutions

5.2. Single Ply Error Detection

To evaluate the sensitivity of specimen with one ply error, we have used two specimens (Specimen $[(0/90)_{12}]_s$, with no error and Specimen $[(0/90)_{12}]_s$ with the 24th ply at 0° instead of 90°). So it was desired to determine if the test had the sensitivity to determine an orientation error of one ply in a forty-eight ply laminate. Two laminates were fabricated for this purpose: Specimen $[(0/90)_{12}]_s$, with no error and Specimen $[(0/90)_{12}]_s$ with ply error. Experimental results for specimen with no error and specimen with ply error is plotted in Fig. 8. Computer simulations were not performed on these samples. Results from the figure indicate that the test has the sensitivity to detect an error of one ply in forty-eight.

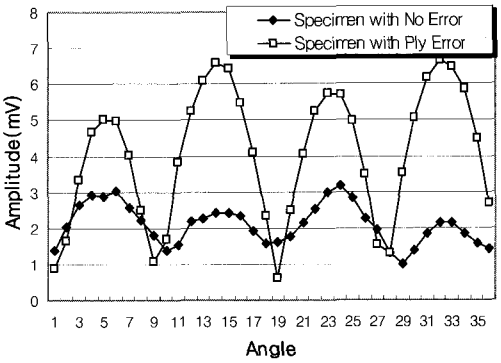

Fig. 8 Comparison of specimen $[(0/90)_{12}]_s$, with no error and specimen $[(0/90)_{12}]_s$ with ply error.

5.3. Experimental Solutions and Theoretical Modeling

A polar scan experimentation was performed using a through transmission and pulse-echo measurement modes with the transducers in a crossed arrangement, that is, the receiver polarization is oriented at 90° to the polarization of the transmitter in the through transmission. For an isotropic material, this test will produce a null, or zero received signal at any transmitter orientation. However, for a laminate consisting

of orthotropic plies, this test is very sensitive to fiber orientation and ply sequence as shown by both the computer modeled and experimental results. The specimens used for this test are based on a realistic layup sequence used in manufacturing composite components and possible errors which can occur during fabrication. When the fixture is assembled for experimental data acquisition by first placing the test specimen face down on the transmitter face plate and aligning its 0^0-90^0 axis between two transducers, it is found that the results was very sensitive with the aligned angle of 90^0 between the transmitter and receiver in the through-transmission method. Also the acousto-ultrasonic technique was used and a simple jig was developed by placing two transducers on one side of sample and measuring the time-of-flight as the function of the separation distance.

Specimens with 0°, 5°, 15° and 20° defect angles were compared to demonstrate the test's capability and sensitivity in determining a misoriented ply or an unsymmetrical layup with the same base sequence as a symmetrical layup with the experimental and theoretical results shown in Figs. 9, 10, 11 and 12. First of all, in the case of specimen with 0° defect angle in the form of symmetric layups, experimental and theoretical solutions were well agreed to some degree. Also experimental acousto-ultrasonic data shows a good agreement compared to the shear wave modeling. Especially peak values are well agreed between modeling, shear wave and acousto-ultrasonic data. Figure 10 shows comparisons of experimental and theoretical results in the case of specimen with 5° defect angle in the form of symmetric layups. So it is found that there exists a good agreement in the amplitude and angle between experimental and theoretical results. Figure 11 shows comparisons of experimental and theoretical results in the case of specimen with 15° defect angle in the form of symmetric layups. Again, some strong correlation is observed in this figure. However there is some difference on the third and fourth peak values between modeling and acousto-ultrasonic data. Fig. 12 shows also shows some difference on the second and third peak values between modeling and acousto-ultrasonic data. It is thought that the acousto-ultrasonic data were manually acquired and affected by the coupling and couplant conditions. There are movements of peak values as the function of amplitude as the defect angle varies. It is thought that peak location of amplitude is related due to the fiber direction of CFRP laminates. There is peak amplitude at about 45 degree in Fig. 9. Here there are peak amplitudes at about 40 degree in Figs. 10-12. It seems that those peaks are almost similar. However there are some difference between them. It is thought that the more detailed data is needed to bring the more exact solution.

Also there are similar situations on acousto-ultrasonic results over those of shear waves. Those data is going up and down regularly. It is thought that the fiber direction of CFRP laminates affected to acousto-ultrasonic signals. We can obtain more big amplitude signal at two transducers on the fiber direction; however on the fiber reverse direction we may get much more small amplitude signal in testing CFRP laminates. So four peaks were found at Figs. 9-12 compared with those of shear wave experimentation.

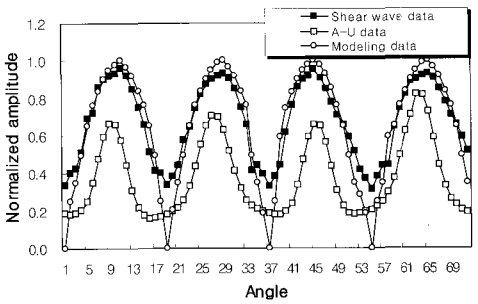

Fig. 9 Comparison of modeling and experimental solutions for 0° defect angle specimen

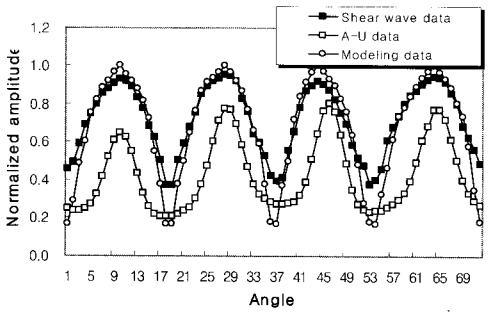

Fig. 10 Comparison of modeling and experimental solutions for 5° defect angle specimen

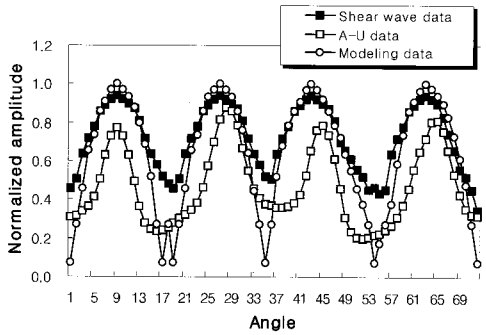

Fig. 11 Comparison of modeling and experimental solutions for 15° defect angle specimen

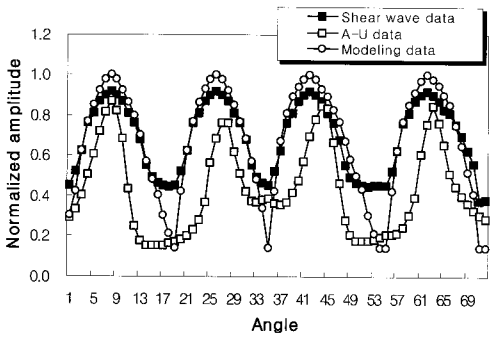

Fig. 12 Comparison of modeling and experimental solutions for 20° defect angle specimen

Experimental data was obtained by placing the transducers on each sample with a viscous /gel couplant, orienting the transmitter, crossing the receiver's orientation such that a minimum peak-to-peak amplitude was displayed on the oscilloscope, and measuring the peak-to-peak amplitude of the minimized signal. This was done for transmitter orientations from 0^0 to 360^0 in 0.9 or 5^0 increments. The results for the experimental and modeling data are graphed in Figs 9, 10, 11 and 12 for comparing difference between test and model. Modeling results were obtained by implementing the simplified ply-by-ply vector decomposition model. A program was written to compute the reference signal coefficients for any transducer and ply orientations, multiply the coefficients by their respective reference signal, combine the resultant signals to model a received signal, and compute the peak-to-peak amplitude of the synthesized signal. Since the dominant signal segments of $R[0_{33}/90_0]$ and $R[0_0/90_{33}]$ are approximately of the same shape and size, the required 32 reference signals were assembled by linearly interpolating the previously obtained $R[0_{33}/90_0]$ reference signals through 33 time shifts. Each sample's layup sequence was entered, and the program computed the peak-to-peak values for the modeled signal for transmitter angles ranging from 0^0 to 360^0 in 0.9 or 5^0 increments with the receiver oriented at $+90^0$ with respect to the transmitter. The modeling and testing results presented here for further research efforts to use ultrasonic shear waves to characterize ply misorientations in composite laminates fabricated from unidirectional plies. Probably the most obvious direction for future research is to solve the inverse problem; that is, given a laminate with a known number of plies, determine the orientation of each ply using the ply-by-ply vector decomposition model.

Those results show a strong qualitative agreement between the experimental and modeling solutions. The data in each plot was normalized by dividing it by the smallest peak-to-peak amplitude value contained in the data for each respective plot. The motorized system had brought the effect of changing couplant conditions to be minimized from test to test which has a significant effect on the amplitude of the received signal. Also rapid scan experimentation can be made to find a defect angle contained in the CFRP composite laminates.

6. Summary and Conclusions

A motorized, PC-controlled ultrasonic scanner and acousto-ultrasonic jig for contact mode in the shear wave transmission and pulse echo method, have been designed and built for NDE of anisotropic composite plates. The contact mode motorized systems have been used to determine the fiber defect angle on graphite epoxy laminates. The systems have been tested on unidirectional graphite epoxy laminate and a good agreement between the experiment and model was obtained. Especially, it was attempted to detect defect angles for symmetric laminates about the mid-defect plane, i.e. $[2(90_3,0_3),90_3,\theta_3,90_3,2(0_3,90_3)]$. To this end a through-transmission ultrasound test method has been performed to evaluate the defect angles of CFRP composite laminates. Both modeling and experimental results demonstrated high sensitivity of the method. In the case of a specimen with using acousto-ultrasonic technique, a little difference was shown between experimental and modeling solutions. It is thought that the acousto-ultrasonic data were manually acquired and affected by the coupling and couplant conditions. And there exists a good agreement between experimental and modeling results in the case of a specimen with 0°, 5°, 15° and 20° defect angles. This high sensitivity is good for characterizing the defect angles in a laminate and detecting real manufacturing errors. And the implementation of the simplified ply-by-ply vector decomposition model has been successfully utilized to qualitatively model the behavior of ultrasound waves transmitted through a composite laminate fabricated from unidirectional plies. This model has the capability to qualitatively predict the effects of a ply misorientation and layup symmetry, as demonstrated by comparing the theoretical and experimental results. Also, ultrasound shear waves require a highly viscous couplant between the transducer and the test piece. The usual shear wave couplant is burnt honey; unfortunately, it is very difficult to maintain a consistent property for burnt honey. Experimental measurement results could not be duplicated with a high degree of quantitative reproducibility due to the inconsistency of the couplant from test to test. However, the results could be reproduced to some degree because of the motorized system. So there are advantages using the scanner which are very useful to find a fiber misorientation of CFRP laminates. Also we can have data based on a function of angle using one-side and both side measurement.

Acknowledgment

This work was aided by the Center for Nondestructive Evaluation and the Institute for Physical Research and Technology at Iowa State University. This study was supported by Factory Automation Research Center for Parts of Vehicles (FACPOV) in Chosun University, Kwangju, Korea. FACPOV is designated as a Regional Research Center of Korea Science and Engineering Foundation (KOSEF) and Ministry of Science and Technology (MOST) operated by Chosun University.

References

Fisher, B. A. and Hsu, D. K. (1996) Application of Shear Waves for Composite Laminate Characterization, *Review of Progress in Quantitative Nondestructive Evaluation*, Vol 15, D. O. Thompson and D. E. Chimenti editors, Plenum Press, New York, 1191-1198

Hale, R.D., Hsu, D.K. and Adams, D.O. (1996) Ultrasonic NDE Techniques and the Effects of Flaws on Mechanical Performance in Multi-Directionally Reinforced Textile Composite, *Review of Progress in Quantitative Nondestructive Evaluation*, Vol. 15, Plenum Press, New York , pp. 1247-1254

Hsu, D. K. (1994) Material Properties Characterization for Composites Using Ultrasonic Methods, *proceeding of Noise-Con 94*, pp. 821-830

Hsu, D. K. and Fei, D (2000) EMAT-generated shear wave transmission for NDE of Composite laminates, *Review of Progress in Quantitative NDE*, edited by D. O. Thompson and D. E Chimenti, AIP, New York, Vol. 19, pp. 1159-1166

Fisher B. A. and Hsu D. K. (1996) Application of Shear Waves for Composite Laminate Characterization, *Review of Progress in Quantitative Nondestructive Evaluation*, Vol 15, D. O. Thompson and D. E. Chimenti editors, Plenum Press, New York, pp. 1191-1198

Hsu, D. K. Fisher, B. A. and Koskamp, M. (1997) Shear Wave Ultrasonic Technique as an NDE Tool for Composite Laminate Before and After Curing, *Review of Progress in Quantitative Nondestructive Evaluation*, Vol 16, D. O. Thompson and D. E. Chimenti editors, Plenum Press, New York, pp. 1975-1982

Hsu, D. K. and Margetan, F. J. (1993) Examining CFRP Laminate Layup with Contact-mode Ultrasonic Measurements, *Adv. Comp. Lett.*, Vol. 2, No. 2, pp. 51-55

Im, K. H., Hsu, D. K., Cho, Y. T., Park, J. W., Sim, J. K. and Yang I. Y. (2002) Characterization of CFRP Laminates' Layups Using Through-Transmitting Ultrasound Waves, *KSME International Journal*, Vol. 16, No. 3, pp. 292-301

Komsky, I. N., Daniel I. M. and Lee C.-Y (1992) Ultrasonic Determination of Layer Orientation in Multilayer Multidirectional Composite Laminates, *Review of Progress in QNDE*, Vol. eds. D. O. Thompson and D. E. Chimenti, Plenum, New York, pp. 1615-22

Komsky, I. N., Zgonc K., and Daniel I. M. (1994) Ultrasonic Determination of Layer Orientation in Composite Laminates Using Adaptive Signal Classifiers, *Review of Progress in QNDE*, Vol. 13, eds. D. O. Thompson and D. E. Chimenti, Plenum, New York, pp. 787-94

Tippler, P. A. (1982), *Physics*, Second Edition, Worth, New York, pp. 863-70

Urabe, K. and Yomoda S. (1982) Non-Destructive Testing Method of Fiber Orientation and Fiber Content in FRP Using Microwave, *Progress in Science and Engineering of Composites*, eds. T. Hayashi, K. Kawata, and S. Umekawa, Japan Society for Composite Materials, Tokyo, pp. 1543-50

Urabe, K. and Yomoda S. (1987) Nondestructive Testing Method of Fiber Orientation in Fiber Reinforced Composites by Microwave, Bulletin of Industrial Products Research Institute, No. 107, pp. 11-21

Urabe, K. (1987) Rotative Polarization System of Millimetric Wave for Detection of Fiber Orientation in CFRP", Bulletin of Industrial Products Research Institute, No. 107, pp. 23-31

Vary, A. (1988) Acousto-Ultrasonics: Theory and Application, Edited by Duck, J.C., Pleum